Diagnostic performance and safety of ultrasound-guided core-needle biopsy for suspicious malignant lymphadenopathy in oncologic staging: A single-center study

L. Wang[1,2], W. Zhao[1*], W. Shi[2], N. An[2], S. Zhang[2]

[1]*Shanxi Provincial People's Hospital(The Fifth Clinical Medical College of Shanxi Medical University), Shanxi Medical University, Taiyuan, China*

[2]*Department of Ultrasound, Yangquan First People's Hospital, Yangquan, Shanxi Province, China*

► ***Original article***

Corresponding author:
Zhao Wenli, M.D.,
E-mail: *17635306222@163.com*

Received: June 2026
Final revised: July 2026
Accepted: July 2026

Int. J. Radiat. Res., October 2026; 24(4): 961-968

DOI: 10.61186/ijrr.24.4.5

Keywords: *Ultrasonography, biopsy, large-core needle, lymph nodes, neoplasm staging, safety.*

ABSTRACT

Background: Pathological confirmation of suspicious lymphadenopathy is essential for oncologic staging and treatment planning. This study evaluated the diagnostic performance and safety of a standardized ultrasound-guided core-needle biopsy (CNB) protocol for suspicious malignant lymphadenopathy. ***Materials and Methods:*** This single-center diagnostic accuracy study included 328 adults who underwent ultrasound-guided core-needle biopsy (CNB) at Yangquan First People's Hospital between January 2021 and June 2023. A standardized workflow was used for ultrasound assessment, route planning, real-time Doppler-assisted guidance, specimen handling, and postprocedural surveillance. Saline-assisted hydrodissection was applied for vascular-adjacent lymph nodes. Final diagnosis was established using surgical pathology, repeat biopsy, immunohistochemistry, microbiological confirmation, or at least 6-month clinical/imaging follow-up. ***Results:*** Technical success was achieved in 317 of 328 patients (96.6%). Among technically successful cases, 175 malignant and 142 benign lesions were identified. Diagnostic accuracy was 95.9% (304/317), sensitivity 96.6% (169/175), specificity 95.1% (135/142), positive predictive value 96.0% (169/176), and negative predictive value 95.7% (135/141). The area under the receiver operating characteristic curve was 0.983 (95% confidence interval [CI], 0.972-0.994). Complications occurred in 14 patients (4.4%), with no severe adverse event. ***Conclusion:*** Standardized ultrasound-guided CNB is a safe and accurate minimally invasive approach for suspicious malignant lymphadenopathy and can support pathological confirmation for oncologic staging and treatment decision-making.

INTRODUCTION

Lymph nodes are key components of the immune and lymphatic systems and are frequently involved in inflammatory disease, granulomatous infection, lymphoma, and metastatic malignancy. In patients with known or suspected cancer, accurate characterization of lymphadenopathy is particularly important because nodal status may determine tumor stage, treatment strategy, radiotherapy target delineation, systemic therapy selection, and prognosis. Imaging findings can suggest malignancy, but histopathological confirmation is often required when imaging features are equivocal, when lymphoma is suspected, or when treatment decisions depend on nodal pathology [1, 2]. Recent studies published in the International Journal of Radiation Research have also emphasized the clinical importance of lymph-node imaging in tumor-imaging and radiotherapy pathways, including cervical metastatic lymphadenopathy, papillary thyroid carcinoma cervical lymph-node metastasis, and nodal staging before radiotherapy [3-6].

Open surgical excision remains diagnostically valuable, especially for lymphoma subtyping, but it is more invasive, requires greater perioperative resources, and may not be suitable for deep or anatomically complex lymph nodes. Fine-needle aspiration is minimally invasive but may provide insufficient tissue architecture for immunohistochemistry and lymphoma classification. Ultrasound-guided core-needle biopsy (CNB) offers real-time visualization, targeted sampling, avoidance of major vessels, and acquisition of tissue cores for histopathology and ancillary testing. For oncologic imaging and staging practice, this technique may bridge the gap between noninvasive imaging and surgical pathology [7-10].

Although ultrasound-guided CNB is widely used in clinical practice, its diagnostic yield and safety depend strongly on target selection, puncture-route planning, needle visualization, specimen handling, and management of vascular-adjacent lesions. Published experience with ultrasound-guided biopsy, ancillary testing, saline-assisted access, and complication management supports the need for a

[DOI: 10.61186/ijrr.24.4.5]

standardized, reproducible protocol [11-14].

This study evaluated the diagnostic performance and safety of a standardized ultrasound-guided CNB protocol in adult patients with suspicious malignant lymphadenopathy. The study focused on technical success, diagnostic accuracy against a composite reference standard, specimen adequacy, complications, and technical risk factors for puncture failure. To improve alignment with tumor imaging and oncologic staging, the analysis emphasized lymph nodes requiring pathological confirmation for suspected metastatic cancer, lymphoma, or treatment-planning decisions. The novelty of this work is the evaluation of a reproducible ultrasound-guided CNB workflow that integrates Doppler-assisted route planning, selective saline-assisted hydrodissection for vascular-adjacent nodes, standardized specimen handling, and a composite reference standard in a large oncologic staging cohort.

MATERIALS AND METHODS

Study design and ethics

This was a single-center diagnostic accuracy study conducted at the Department of Ultrasound, Yangquan First People's Hospital, Shanxi Province, China. The study included consecutive eligible adult patients who underwent ultrasound-guided CNB for suspicious lymphadenopathy between January 2021 and June 2023. The study was approved by the Institutional Review Board of Yangquan First People's Hospital (registration/approval No. YQDYRMYY-LL-2020-101; approval date: 29 December 2020). Written informed consent was obtained before the procedure. Patient information and images were anonymized in accordance with institutional privacy requirements and the principles of the Declaration of Helsinki.

Study population

A total of 328 patients were enrolled. Eligible patients were aged 18 years or older and had lymph nodes requiring pathological confirmation because of suspected malignant involvement, lymphoma, or clinically unresolved lymphadenopathy in an oncologic diagnostic pathway. Target sites included cervical, supraclavicular, axillary, inguinal, and abdominal lymph nodes. Sonographic inclusion criteria were a superficial short-axis diameter of 8 mm or greater or a deep short-axis diameter of 10 mm or greater, and at least one suspicious sonographic feature, including loss of the echogenic hilum, asymmetric cortical thickening greater than 3 mm, cystic or necrotic change, microcalcification, rounded morphology, or abnormal mixed/peripheral vascular distribution.

Exclusion criteria were uncorrectable coagulopathy (international normalized ratio >1.5 or platelet count <50 × 10^9/L), lack of a safe ultrasound-visible puncture route, active infection or skin disruption along the puncture path, inability to tolerate the required position, pregnancy, or previous radiotherapy to the target lymph-node region when it could substantially confound local anatomy or procedural safety assessment.

Ultrasound imaging equipment, materials, and biopsy system

Ultrasound examinations and procedures were performed using a Mindray Kunlun 7 color Doppler ultrasound system with a high-frequency linear probe (L18-5, 5-18 MHz) and a convex probe (C9-2, 2-9 MHz) (Mindray Bio-Medical Electronics Co., Ltd., Shenzhen, China). The linear probe was used for superficial lymph nodes with a depth of 3 cm or less, and the convex probe with harmonic imaging was used for deeper lymph nodes. Color Doppler and microvascular imaging were used to evaluate vascular distribution and to select a safe needle path. Gain, wall filter, pulse repetition frequency, depth, and focus were adjusted individually to optimize visualization while avoiding artifactual flow signals. No magnetic resonance imaging (MRI), computed tomography (CT)-guided biopsy, contrast-enhanced ultrasound (CEUS), or ultrasound contrast agent was used in this protocol.

All procedures were performed using an 18-gauge disposable semi-automatic core biopsy needle (A-type, 1.2 mm [18G] × 160 mm, REF 11101201; LEAPMED Medical, Suzhou Lipu Medical Technology Co., Ltd., Suzhou, China). Local anesthesia was performed with 1% lidocaine hydrochloride injection; hydrodissection used sterile 0.9% normal saline; and tissue fixation used 10% neutral-buffered formalin. No contrast agents were used. The sampling length was adjusted according to lymph-node size and the available safe path. The same needle gauge was used throughout the study to minimize heterogeneity in diagnostic yield and complication assessment.

Standardized ultrasound-guided CNB procedure

The standardized workflow consisted of four steps: preprocedural assessment, puncture-route planning, real-time guided biopsy, and specimen processing.

First, the patient was positioned to expose the target lymph node. Multiplanar ultrasound scanning was performed to measure long-axis and short-axis diameters, depth from the skin, relationship to adjacent vessels and nerves, echogenic hilum, cortical morphology, necrotic or cystic areas, and vascular distribution. Elastography was used when available to help avoid predominantly necrotic areas and to target solid portions of the lymph node.

Second, the puncture point and needle route were planned according to the shortest safe path that

[DOI: 10.61186/ijrr.24.4.5]

avoided major vessels, nerves, lung apex, bowel, and necrotic areas. Local anesthesia was administered with 5 mL of 1% lidocaine from the skin to the tissue surrounding the target. For lymph nodes adjacent to major vessels, saline-assisted hydrodissection was performed by slowly injecting 3-5 mL sterile normal saline between the lymph node and the adjacent vessel under real-time ultrasound guidance. The biopsy route was used only after a temporary liquid separation zone was confirmed.

Third, the needle was advanced freehand under continuous real-time ultrasound visualization. The needle tip was kept within the imaging plane whenever possible. For superficial lymph nodes, a shallow approach of approximately 10-15 degrees was preferred; for deep lymph nodes, the angle was adjusted according to target depth and safe-route feasibility. One to three puncture passes were performed according to specimen length, target accessibility, and real-time tissue-core quality. Necrotic or cystic areas were avoided. After sampling, the puncture site was compressed for at least 5 minutes, and ultrasound re-examination was performed after 30 minutes to exclude active bleeding or hematoma formation.

Fourth, tissue cores were immediately placed in 10% neutral-buffered formalin, labeled, and sent to the Department of Pathology within 30 minutes. Samples were visually assessed for core integrity and length. Immunohistochemistry (IHC), microbiological testing, or additional pathological consultation was performed when clinically indicated, especially for suspected lymphoma or granulomatous disease.

Pathological investigation was performed by two experienced pathologists who were not involved in the ultrasound-guided procedure. Tissue cores were fixed, paraffin embedded, sectioned at approximately 4 μm, and stained with hematoxylin and eosin. IHC panels were selected according to morphology and clinical suspicion: metastatic carcinoma was evaluated using epithelial and site-specific markers when required; suspected lymphoma was assessed using lymphoid lineage, germinal-center, and proliferation markers; and granulomatous disease was assessed using special staining, microbiological tests, or clinicopathological correlation when indicated. Discordant or indeterminate diagnoses were resolved by consensus review and correlation with repeat biopsy, surgery, microbiology, or follow-up.

Reference standard

To avoid incorporation bias, the ultrasound-guided CNB result was treated as the index test. The final reference-standard diagnosis was based on surgical pathology when available, repeat biopsy, immunohistochemistry with clinicopathological consensus, microbiological confirmation, or at least 6 -month clinical and imaging follow-up. Cases with persistent diagnostic uncertainty were reviewed by two senior pathologists and the clinical team. Malignancy was defined as metastatic carcinoma or lymphoma confirmed by the reference standard. Benign disease included reactive hyperplasia, granulomatous inflammation including tuberculosis, cat-scratch disease, sarcoidosis-like disease, Castleman disease, and other nonmalignant inflammatory lesions.

Outcome measures

The primary outcome was diagnostic accuracy for malignancy among technically successful biopsies. Diagnostic indices included sensitivity, specificity, positive predictive value, negative predictive value, and area under the receiver operating characteristic curve. Secondary outcomes included technical success, specimen-quality grade, complications within 24 hours, and risk factors for puncture failure.

Technical success was defined as successful needle placement into the target lymph node and acquisition of tissue containing lymph-node material. Specimen quality was graded as follows: Grade A, intact tissue cores of at least 10 mm containing preserved lymphoid architecture or definitive malignant structures; Grade B, diagnostic tissue cores of 5-9 mm with partial tissue fragmentation but sufficient for pathological interpretation; and Grade C, limited or suboptimal tissue requiring ancillary testing, repeat pathological review, or correlation with follow-up, but not automatically classified as technical failure. Technical failure was defined as inability to obtain lymph-node tissue because of off-target sampling, severe motion, inaccessible depth, or inadequate visualization.

Statistical analysis

Statistical Package for the Social Sciences (SPSS) version 26.0 (IBM Corp., Armonk, NY, USA) was used for statistical analysis. Continuous variables are presented as mean ± standard deviation or median and range as appropriate. Categorical variables are presented as number and percentage. Diagnostic performance was calculated from a 2 × 2 contingency table and reported with 95% confidence intervals (CIs) when available. Differences between superficial and deep lymph-node groups were assessed using the independent-samples t test for continuous variables and chi-square or Fisher's exact test for categorical variables. Logistic regression was used to identify risk factors for technical failure. Variables included in the model were age, lymph-node depth, short-axis diameter, anatomical site, and vascular-adjacent location. A two-sided P value <0.05 was considered statistically significant.

[DOI: 10.61186/ijrr.24.4.5]

RESULTS

Baseline characteristics

A total of 328 patients were included. There were 176 men (53.7%) and 152 women (46.3%), with a median age of 54 years and an age range of 28-79 years. Target lymph nodes were cervical in 152 cases (46.3%), axillary in 94 cases (28.7%), inguinal in 58 cases (17.7%), and abdominal in 24 cases (7.3%). The mean short-axis diameter was 12.3 ± 3.7 mm. Superficial lymph nodes had a mean depth of 1.8 ± 0.7 cm, whereas deep lymph nodes had a mean depth of 4.6 ± 1.2 cm (P<0.001). Suspicious sonographic findings included loss of the echogenic hilum in 257 cases (78.4%), asymmetric cortical thickening in 214 cases (65.2%), and cystic or necrotic change in 110 cases (33.5%).

Table 1. Baseline characteristics of the study population (n=328). Abbreviations: none.

Characteristic	Value
Sex, male/female	176/152 (53.7%/46.3%)
Age, years	Median 54; range 28-79
Cervical lymph nodes	152 (46.3%)
Axillary lymph nodes	94 (28.7%)
Inguinal lymph nodes	58 (17.7%)
Abdominal lymph nodes	24 (7.3%)
Mean short-axis diameter	12.3 ± 3.7 mm
Superficial lymph-node depth	1.8 ± 0.7 cm
Deep lymph-node depth	4.6 ± 1.2 cm
Loss of echogenic hilum	257 (78.4%)
Asymmetric cortical thickening	214 (65.2%)
Cystic or necrotic change	110 (33.5%)

Technical success and specimen quality

Technical success was achieved in 317 of 328 patients, corresponding to a technical success rate of 96.6%. Eleven cases were classified as technical failures. Nine failures occurred in deep abdominal lymph nodes because of respiratory displacement or insufficient needle-tip stability, and two failures occurred in small cervical lymph nodes with a short-axis diameter less than 8 mm because of needle-path deviation. The mean number of puncture passes was 1.4 ± 0.6 (range, 1-3). Deep lymph nodes required more passes than superficial lymph nodes (2.1 ± 0.8 vs. 1.2 ± 0.4, P<0.001). Representative anonymized ultrasound images with arrows marking the target region of interest (ROI) are shown in figures 1-5.

Among 317 technically successful biopsies, specimen quality was Grade A in 198 cases (62.5%), Grade B in 99 cases (31.2%), and Grade C in 20 cases (6.3%). Grade C samples were mainly observed in lymph nodes deeper than 4 cm or in nodes with necrotic components exceeding 50% of the target region. Logistic regression showed that depth greater than 3 cm (odds ratio [OR]=4.27, 95% CI 2.15-8.49, P<0.001) and short-axis diameter less than 10 mm (OR=3.18, 95% CI 1.72-5.88, P<0.001) were independent risk factors for technical failure.

Table 2. Technical success, specimen quality, and risk factors. Abbreviations: CI, confidence interval; OR, odds ratio.

Parameter	Result
Technical success	317/328 (96.6%)
Technical failure	11/328 (3.4%)
Mean number of passes	1.4 ± 0.6; range 1-3
Deep vs. superficial pass number	2.1 ± 0.8 vs. 1.2 ± 0.4; P<0.001
Grade A specimen	198/317 (62.5%)
Grade B specimen	99/317 (31.2%)
Grade C limited specimen	20/317 (6.3%)
Depth >3 cm as failure risk factor	OR=4.27; 95% CI 2.15-8.49; P<0.001
Short-axis diameter <10 mm as failure risk factor	OR=3.18; 95% CI 1.72-5.88; P<0.001

Final pathological classification

Among the 317 technically successful cases included in the diagnostic-performance analysis, the final reference standard identified 175 malignant lesions (55.2%) and 142 benign lesions (44.8%). Malignant lesions included 120 metastatic carcinomas and 55 lymphomas. The most common metastatic primary tumors were lung adenocarcinoma, breast cancer, and gastric cancer. Lymphoma subtypes included diffuse large B-cell lymphoma, follicular lymphoma, and Hodgkin lymphoma. Benign lesions were mainly reactive hyperplasia and granulomatous inflammation, including tuberculous granuloma. A small number of cases were classified as cat-scratch disease, sarcoidosis-like disease, Castleman disease, or other inflammatory lesions after clinicopathological correlation.

Table 3. Final reference-standard pathological classification among technically successful cases (n=317). Abbreviations: none.

Category	Pathological type	Number	Percentage within category
Benign	Reactive hyperplasia	89	62.7%
Benign	Granulomatous inflammation including tuberculosis	38	26.8%
Benign	Other inflammatory diseases	15	10.6%
Malignant	Metastatic carcinoma	120	68.6%
Malignant	Lymphoma	55	31.4%
Metastatic carcinoma	Lung adenocarcinoma	42	35.0%
Metastatic carcinoma	Breast cancer	37	30.8%
Metastatic carcinoma	Gastric cancer	21	17.5%
Metastatic carcinoma	Other primary tumors	20	16.7%
Lymphoma	Diffuse large B-cell lymphoma	32	58.2%
Lymphoma	Follicular lymphoma	12	21.8%
Lymphoma	Hodgkin lymphoma	8	14.5%

Diagnostic performance for malignancy

The diagnostic-performance analysis was based on 317 technically successful biopsies. According to the final reference standard, there were 175 malignant and 142 benign lesions. Ultrasound-guided

[DOI: 10.61186/ijrr.24.4.5]

CNB correctly identified 169 malignant lesions and 135 benign lesions. There were 7 false-positive and 6 false-negative results. Overall diagnostic accuracy was therefore 95.9% (304/317). Sensitivity was 96.6% (169/175), specificity was 95.1% (135/142), positive predictive value was 96.0% (169/176), and negative predictive value was 95.7% (135/141). The area under the receiver operating characteristic curve (AUC) was 0.983 (95% CI, 0.972-0.994; P<0.001). Subgroup analysis showed that diagnostic performance was slightly higher for metastatic carcinoma than for lymphoma, reflecting the greater need for preserved tissue architecture and immunophenotyping in lymphoma diagnosis.

Table 4. Diagnostic contingency table for malignancy among technically successful cases (n=317). Abbreviation: CNB, core-needle biopsy.

CNB result	Reference-standard malignant	Reference-standard benign
CNB positive for malignancy	169 (true positive)	7 (false positive)
CNB negative for malignancy	6 (false negative)	135 (true negative)

Table 5. Diagnostic performance indices. Abbreviations: AUC, area under the receiver operating characteristic curve; CI, confidence interval; ROC, receiver operating characteristic.

Index	Value
Accuracy	95.9% (304/317; 95% CI, 93.1-97.6)
Sensitivity	96.6% (169/175; 95% CI, 92.7-98.4)
Specificity	95.1% (135/142; 95% CI, 90.2-97.6)
Positive predictive value	96.0% (169/176; 95% CI, 92.0-98.1)
Negative predictive value	95.7% (135/141; 95% CI, 91.0-98.0)
Area under the ROC curve	0.983 (95% CI, 0.972-0.994)
Optimal cut-off in ultrasound score model	0.52 by Youden index

Complications

Fourteen complications were recorded within 24 hours after biopsy, corresponding to an overall complication rate of 4.4% among technically successful cases. Local hematoma occurred in 9 cases (2.8%), with maximum diameter ranging from 1.2 to 2.3 cm; all resolved after compression or conservative management. Transient nerve-related symptoms occurred in 3 cases (0.9%), presenting as numbness of the ipsilateral upper limb after axillary lymph-node biopsy; all resolved within 1 week. Local infection occurred in 2 cases (0.6%) and resolved after oral antibiotics. No major hemorrhage, pneumothorax, permanent nerve injury, or procedure-related death occurred. Hematoma was more frequent in lymph nodes with abundant blood flow than in those with lower vascularity.

Table 6. Postprocedural complications. Abbreviations: none.

Complication	Number	Rate	Outcome
Local hematoma	9	2.8%	Resolved with compression or conservative treatment
Transient nerve symptoms	3	0.9%	Resolved within 1 week
Local infection	2	0.6%	Resolved after oral antibiotics
Major hemorrhage/ pneumothorax/ permanent nerve injury	0	0%	Not observed
Total complications	14	4.4%	No severe adverse event

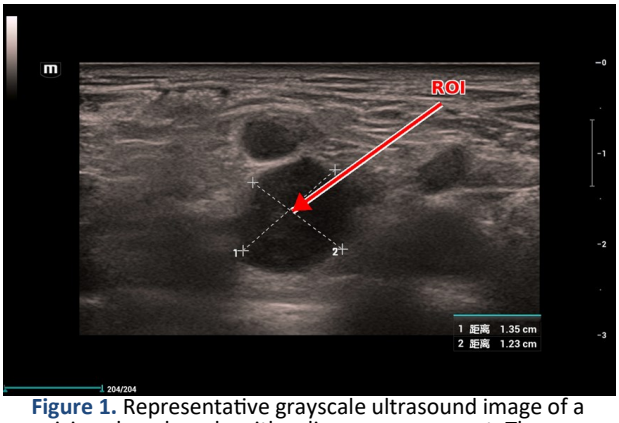

Figure 1. Representative grayscale ultrasound image of a suspicious lymph node with caliper measurement. The arrow indicates the target region of interest (ROI) selected for ultrasound-guided core-needle biopsy (CNB).

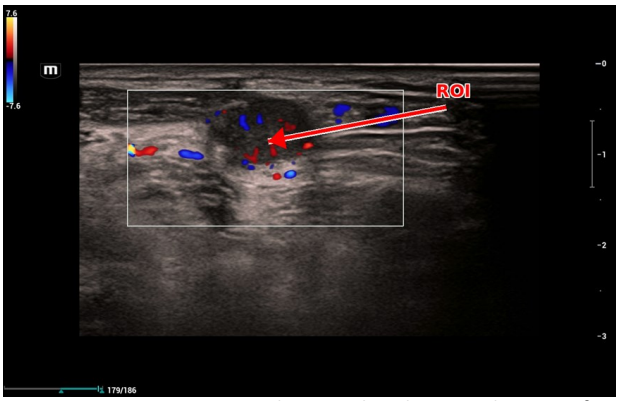

Figure 2. Representative color Doppler ultrasound image of a suspicious lymph node. The arrow indicates the solid target ROI while Doppler imaging demonstrates adjacent and intranodal vascular signals.

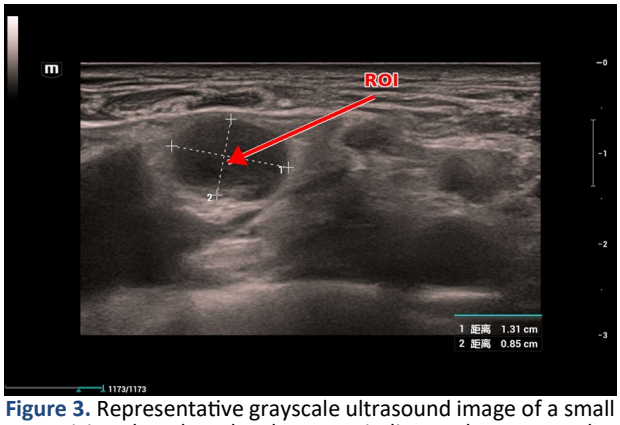

Figure 3. Representative grayscale ultrasound image of a small suspicious lymph node. The arrow indicates the measured target ROI.

[DOI: 10.61186/ijrr.24.4.5]

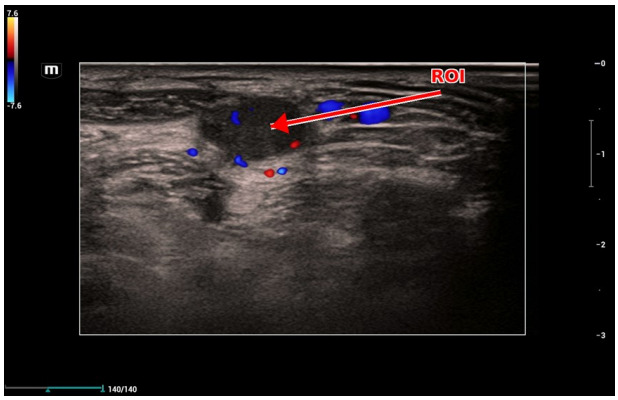

Figure 4. Representative color Doppler ultrasound image used for route planning. The arrow indicates the target ROI selected after assessment of vascular distribution.

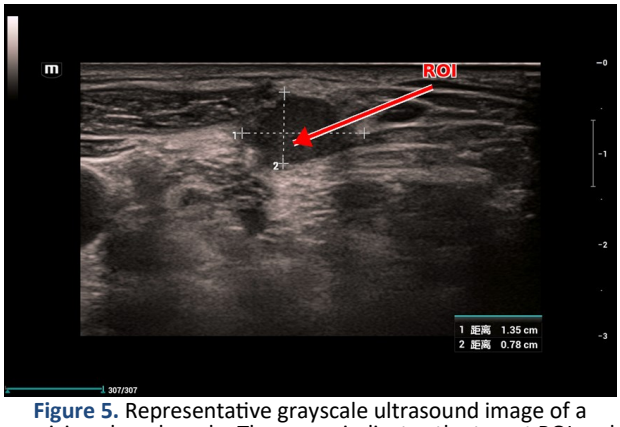

Figure 5. Representative grayscale ultrasound image of a suspicious lymph node. The arrow indicates the target ROI and the measured short-axis region.

DISCUSSION

This single-center study indicates that a standardized ultrasound-guided CNB protocol can provide reliable pathological confirmation for suspicious malignant lymphadenopathy in an oncologic diagnostic setting. Rather than replacing imaging, the procedure complements tumor-imaging and staging workflows by providing tissue for histopathology, IHC, and clinicopathological correlation when imaging alone is insufficient [1-6].

Compared with recent IJRR imaging studies, the present study addresses a complementary tissue-confirmation question. Jia *et al.* reported that CEUS and shear wave elastography (SWE) were useful for differentiating metastatic from tuberculous cervical lymphadenopathy, and Yu *et al.* reported improved diagnostic performance when CEUS was combined with CT for cervical lymph-node metastasis in papillary thyroid carcinoma [3, 5]. Those studies support noninvasive risk stratification, whereas our protocol provides histological confirmation and ancillary testing material; therefore, the high diagnostic performance observed here is clinically plausible and directly relevant when imaging results must be confirmed before oncologic staging or treatment planning.

This study emphasizes oncologic staging and tumor imaging rather than unexplained lymphadenopathy in a broad internal-medicine sense. In patients with suspected or known malignancy, nodal pathology may change the disease stage, determine the need for systemic therapy, guide radiotherapy target definition, or establish lymphoma subtype. Ultrasound-guided CNB is particularly useful for superficial cervical, supraclavicular, axillary, and inguinal nodes, where real-time imaging allows accurate needle placement and avoidance of critical structures. For deeper nodes, technical difficulty increases, but systematic route planning and Doppler-assisted safety assessment can maintain procedural feasibility.

A key methodological feature of this study was the use of a composite reference standard rather than treating the CNB result itself as the gold standard. When the index test and reference standard are not clearly separated, diagnostic accuracy may be overestimated. In this analysis, final diagnosis was based on surgical pathology when available, repeat biopsy, immunohistochemistry, microbiological confirmation, or 6-month clinical/imaging follow-up. This approach better reflects real-world diagnostic practice while reducing incorporation bias.

The standardized workflow may explain the favorable technical success and safety profile. Preprocedural assessment identified lymph-node morphology, depth, vascularity, and necrotic components. Real-time ultrasound guidance allowed needle-tip monitoring, and Doppler imaging helped avoid major vessels. Saline-assisted hydrodissection was used for vascular-adjacent lesions, creating a temporary protective fluid plane between the target and vessel. This maneuver is especially relevant for cervical and axillary lymph nodes, where important vessels and nerves are often close to the target [11-14]. In addition, specimen handling within 30 minutes and early pathological quality assessment improved the likelihood of obtaining diagnostically useful cores.

Deep location and small short-axis diameter were independent risk factors for technical failure. This is clinically plausible because deep abdominal lymph nodes are affected by respiratory motion and needle-angle instability, while small nodes provide a narrow target and are more vulnerable to off-target sampling. In such cases, repeated route planning, respiratory training, alternative patient positioning, and avoidance of necrotic components may improve success. If sufficient tissue cannot be obtained, repeat biopsy or surgical excision should be considered, particularly when lymphoma is suspected.

The diagnostic performance for metastatic carcinoma was slightly higher than that for lymphoma. Metastatic carcinoma often requires identification of malignant epithelial cells and may be reliably diagnosed from small core samples. In contrast, lymphoma diagnosis and subtyping require

[DOI: 10.61186/ijrr.24.4.5]

preservation of tissue architecture, immunophenotyping, and sometimes molecular testing. Therefore, CNB can provide an important preliminary and often definitive diagnosis, but it should not be regarded as a universal replacement for excisional biopsy in all suspected lymphoma cases [8-10].

This study has several limitations. First, it was conducted at a single center, and operator experience may limit generalizability. Second, rare lymph-node diseases were underrepresented. Third, although a composite reference standard was used, not all patients underwent surgical excision, and follow-up-based confirmation may introduce verification bias. Fourth, this study did not directly compare CNB with fine-needle aspiration, endobronchial biopsy, cryo-node biopsy, or CT-guided biopsy, all of which may have roles in selected clinical settings [15-17]. Future multicenter prospective studies should compare different biopsy techniques, evaluate cost-effectiveness, and determine which patient subgroups benefit most from ultrasound-guided CNB.

CONCLUSION

Standardized ultrasound-guided CNB is a safe and accurate method for pathological confirmation of suspicious malignant lymphadenopathy. It provides high sensitivity, specificity, and overall accuracy for distinguishing malignant from benign lymph-node disease and can support oncologic staging and treatment decision-making. Saline-assisted hydrodissection and real-time Doppler-assisted route planning may improve procedural safety for vascular -adjacent lymph nodes. Deep lymph nodes and small short-axis diameters remain important technical challenges and should be addressed through careful patient selection and procedural planning.

***Acknowledgments*:** The authors thank the Department of Pathology and the Department of Ultrasound of Yangquan First People's Hospital for their assistance with specimen processing and clinical data verification.

***Data availability statement*:** The datasets generated and/or analyzed during the current study are available from the corresponding author on reasonable request. The data are not publicly available because of privacy and ethical restrictions concerning patient information. Access is subject to institutional review board approval and applicable data-protection requirements.

***Conflict of interest statement*:** The authors declare that they have no competing interests.

***Funding statement*:** This study received no specific grant from any funding agency in the public, commercial, or not-for-profit sectors.

***Ethical consideration*:** This study was approved by the Institutional Review Board of Yangquan First People's Hospital (registration/approval No. YQDYRMYY-LL-2020-101; approval date: 29 December 2020). Written informed consent was obtained from all participants before biopsy. Patient data and images were anonymized before analysis and manuscript preparation.

***Authors' contribution*:** W.L., contributed to study design, data collection, data analysis, and manuscript drafting. Z.W., contributed to study conception, supervision, methodology review, and critical revision of the manuscript. S.W., A.N., and Z.S., contributed to ultrasound procedures, clinical data collection, specimen tracking, and data verification. All authors reviewed and approved the final manuscript and agree to be accountable for the work.

***AI Usage for manuscript preparation*:** AI-assisted language editing and formatting were used only to improve grammar, readability, structure, and presentation of the revised manuscript and response letter. No AI tool was used to generate original study data, perform statistical analysis, alter clinical image content beyond anonymization and arrow annotation, or draw scientific conclusions. All AI-assisted edits were checked and approved by the authors.

REFERENCES

1. Thong L, Daneshvar C, Hassan M, *et al.* (2026) The role of ultrasound-guided cervical lymph node biopsy in lung cancer: a scoping review. *Respir Investig,* ***64****(1): 101331*.
2. Winkler N, Buxton J, Freer P, *et al.* (2023) Comparison of diagnostic sensitivity and procedure-related pain of concurrent ultrasound-guided fine-needle aspiration and core-needle biopsy of axillary lymph nodes in patients with suspected or known breast cancer. *J Breast Imaging,* ***5****(4): 436-444*.
3. Jia F, Feng S, Song T, Wang X (2026) The diagnostic performance of differentiating cervical metastatic lymphadenopathy and tuberculous nodes by shear wave elastography and contrast-enhanced ultrasonography. *Int J Radiat Res,* ***24****(1): 49-54*.
4. Fan X, Zheng K, Chen W, Zhan L, *et al.* (2023) Ultrasonography features and American college of radiology thyroid imaging reporting and data system category in the prediction of central lymph node metastasis in papillary thyroid carcinoma. *Int J Radiat Res,* ***21****(4): 815-820*.
5. Yu T, Liu L, Wang Z, Li R, *et al.* (2026) Analysis of the value of contrast-enhanced ultrasound with CT imaging in the assessment of preoperative cervical lymph node metastases in papillary thyroid cancer. *Int J Radiat Res,* ***24****(2): 441-447*.
6. Basaran H, Celik C, Bilgi A, *et al.* (2026) Effects of extraperitoneal lymph node dissection vs. imaging methods on survival in staging before radiotherapy in advanced cervical cancer. *Int J Radiat Res,* ***24****(2): 449-456*.
7. Serrano TLDM, Gallardo CMA, Gonzalez VJ, *et al.* (2025) The importance of the interventional pathologist in fine needle aspiration and core needle biopsy procedures for lymph node lesions: a retrospective analysis of diagnostic correlation and proposal of a classification system for lymph node core needle biopsies. *Diagnostics,* ***15****(20): 2628*.
8. Singh N, Mishra S, Balasubramanian P, *et al.* (2025) Comparative analysis on efficacy of lymph node sampling through whole node excision versus core needle biopsy: focusing on diagnostic yield for interpretation. *J Hematopathol,* ***18****(1): 46*.
9. Mogensen HB, Nielsen HT, Pedersen OM, *et al.* (2025) Core needle biopsies in patients with lymphoproliferative malignancies: an observational single-center cohort study. *Eur J Haematol,* ***116****(1): 85-92*.

[DOI: 10.61186/ijrr.24.4.5]

10. Jin X, Jiang H, Jiang Y, *et al.* (2024) Analysis of flow cytometry data from ultrasound-guided lymph node biopsies with two types of needles. *Int J Lab Hematol,* ***46****(5): 869-877*.
11. Reshma G, Ahmad H, Lee KY, *et al.* (2023) Saline-aided ultrasound-guided transoral biopsy of retropharyngeal nodes in head and neck cancer: a feasibility study of five patients. *Head Neck,* ***45****(9): 2355-2362*.
12. Li LH, Ma JJ, Zhou TT, *et al.* (2025) Hot topic: cervical lymph node biopsy and washout thyroglobulin measurement in ultrasound-guided biopsy of thyroid nodules and cervical lymph nodes. *Zhonghua Nei Ke Za Zhi,* ***64****(6): 499-503*.
13. Li LH, Ma JJ, Zhou TT, *et al.* (2025) Hot topic: indications for molecular testing in ultrasound-guided biopsy of thyroid nodules and cervical lymph nodes. *Zhonghua Nei Ke Za Zhi,* ***64****(5): 377-384*.
14. Li LH, Ma JJ, Zhou TT, *et al.* (2025) Hot topic: complications and management in ultrasound-guided biopsy of thyroid nodules and cervical lymph nodes. *Zhonghua Nei Ke Za Zhi,* ***64****(4): 283-287*.
15. Ficoto FL, Junior CJD, Nora RG, *et al.* (2025) Applicability of fine-needle aspiration biopsy of lymph nodes using WHO reporting system: comparison between pediatric and adult Brazilian populations. *Acta Cytol, 1-22*.
16. Yu XW, Zhan FF, Hong YP, *et al.* (2025) Atypical sarcoidosis diagnosed using endobronchial ultrasound-guided mediastinal lymph node biopsy with fine biopsy forceps: two case reports. *World J Clin Cases,* ***13****(32): 111525*.
17. Madan M, Kumar R, Ish P, *et al.* (2025) Additional yield of transbronchial cryo-node biopsy over endobronchial ultrasound-guided transbronchial needle aspiration for mediastinal lesions at a tertiary care center in India. *Monaldi Arch Chest Dis,* ***95****(2)*.

[DOI: 10.61186/ijrr.24.4.5]